



Elastic Behavior of Lead Germanate Near Transition Temperature

I. J. Abdul Ghani

Department of Physics, College of Education Ibn Al-Haitham, University of Baghdad

Received in: 15 April 2012 Accepted in: 9 December 2012

Abstract

All the stiffened and unstiffened elastic constants for lead germanate ($\text{Pb}_5\text{Ge}_3\text{O}_{11}$) single crystal have been measured from room temperature 298 K up to 513K by using ultrasonic pulse superposition technique. The correction of piezoelectric stiffening has been used to obtain the unstiffened elastic constants. Elastic moduli of lead germanate (C_{11} , C_{33} , C_{12} , C_{13} , C_{44} and C_{66}) decrease with the increase of temperature. C_{11} , C_{33} , C_{12} and C_{13} suffered a dip at transition temperature but they increase with the increase of temperature just above Curie temperature between 453 and 473 K because of their positive temperature coefficients in this range, and then decrease slightly (except C_{12} increases) in the range between 473K and 513K. But for the shear elastic moduli (C_{44} and C_{66}): C_{44} shows very slight and gradual increase and then decrease with the increase of temperature, while C_{66} shows a small and graduate decrease with increasing temperature. These measurements were compared with previous experimental published work.

Keywords: Lead germanate, Elasticity, Phase transition, Optical activity, Piezoelectric crystal

Introduction

Lead germanate single crystal ($\text{Pb}_5\text{Ge}_3\text{O}_{11}$) is both ferroelectric [1,2] and optically active below Curie temperature $T_c = 450$ K [3-5]. In several biaxial ferroelectrics optical activity has been observed, but is the only uniaxial ferroelectric studied in detail. Lead germanate undergoes ferroelectric phase transition with emerging of spontaneous polarization along the unique trigonal [6]. Lead germanate single crystal is ambidextrous; [7] below Curie point (450 K) the handedness of the optical activity inverse when the spontaneous polarization is reversed by an applied electric field. Both the optical activity and the spontaneous electric polarization disappear at the Curie temperature [8,9]. At $T_c = 450$ K lead germanate undergoes a second order phase transition from the paraelectric to the ferroelectric phase [5,9] which gives rise to very rapid changes of polarization P with temperature just below T_c . The Curie temperature decreases toward room temperature with uniaxial pressure [10] and doping of germanium in $\text{Pb}_5\text{Ge}_3\text{O}_{11}$ by Si or Ba [11,12]. Measurements of polarization as a function of temperature confirmed the shift in the transition temperature [11]. Lead germanate is not of interest as an acousto-optic material [13] or as a transducer since electromechanical coupling factors are small [14] and ultrasonic attenuation is large [13] but the electro-optic coefficients shows more promise [15,16].

By applying resonance technique Yamada et al. [14] have measured the values of all elastic, dielectric and piezoelectric constants at room temperature, as well as the temperature dependence of the elastic compliance S_{11}^E and of the two piezoelectric constants d_{31} and d_{22} . Both S_{11}^E and d_{31} show upward directed cusp-like anomalies near T_c , but d_{22} is approximately independent of temperature [14]. Both in the ferroelectric and in the paraelectric phases, the



dielectric constant ϵ_{33} follows a Curie-Weiss law [2,17], but ϵ_{11} is only weakly temperature dependence. Several soft Raman active modes have been observed [18,19] which decrease with temperature in a manner so as to lead Lyddane-Sachs-Teller relation via to the Curie-Weiss law for ϵ_{33} [17].

Second order elastic constants (SOEC) of lead germanate single crystal at room temperature have been calculated [14,20]. The purpose of this work is to report experimental data on all elastic constants (stiffened and unstiffened) versus temperatures from room temperature 298 to 513 K, and to compare the results with previous published work of Barsch et al. [21].

At room temperature $\text{Pb}_5\text{Ge}_3\text{O}_{11}$ belongs to the $R\bar{3}^-$ Laue group, crystals of which have a more complicated elastic behavior than those belonging to the higher symmetry $R\bar{3}m$ Laue group. There are seven independent elastic moduli: C_{11} , C_{33} , C_{44} , C_{12} , C_{13} , C_{14} and C_{25} . The point symmetry changes to $\bar{6} = 3/m$ (C_{3h}) at phase transition, decreasing the number of independent elastic constants from seven to five: C_{11} , C_{33} , C_{44} , C_{12} , and C_{13} [21]. Above Curie point, C_{14} and C_{25} are zero.

In ferroelectric state (below Curie temperature) lead germanate crystals contain 180° domains. In this work unpoled crystals were used which twinned on a very fine scale too small to be seen optical. Because of twinning, the effective symmetry is $\bar{6}$, rather than 3, so that the elastic constants C_{14} and C_{25} are absent in unpoled lead germanate, both above and below the transition temperature. Because C_{14} and C_{25} are very small, it makes very little difference whether measurements are made on single-domain specimens or not. Room temperature measurements on single-domain $\text{Pb}_5\text{Ge}_3\text{O}_{11}$ gave $C_{14} = 0.004 \times 10^{10} \text{ N.m}^{-2}$ and $C_{25} = 0.00$, more than twenty times smaller than the other five elastic constants [20].

Till today, very limited experimental data are available in literature on the measurements of the elastic constants of lead germanate at different temperatures, due to the complicated and unique structure of this crystal; its structure changes from ferroelectric rhombohedral below Curie temperature to paraelectric hexagonal above Curie temperature.

Experimental procedure

Good optical-quality large single crystalline boules of $\text{Pb}_5\text{Ge}_3\text{O}_{11}$ grown by Czochralski method, and well-characterized growth defect [22] with density value of 7390 kg.m^{-3} . Platelets of the crystal about 3 to 5 mm thick with orientations in [100], [001] and in direction of 45° to these crystallographic axes were prepared. For ultrasonic measurements, gold plated quartz transducers X (longitudinal) and Y (shear) cut transducers with resonance frequency of 10 MHz and with diameters of 6 mm and 4 mm have been used [23] were cemented to specimen with non-aqueous stopcock grease and also phenyl salicylate have been found to be suitable for bonding at room temperature, but above 473 K (Exempt 9901 lubrication Engineering Co.) is superior as a bond material.

A pulse echo overlap system is used to measure the ultrasonic wave transit time [21,23,24] the travel times of 20 MHz longitudinal and transverse waves were measured for eight different modes at 5 deg intervals from 323 to 523 K, except near transition temperature where data were taken in 1 deg increments. In the vicinity of the transition ultrasonic attenuation was found to increase considerably. Errors from thermal gradients and temperature measurements were smaller than 0.3 deg.

Results

In Table 1, the relations for the stiffened elastic constants $C_{\mu\nu}' = \rho V^2$ (V is actual ultrasonic velocity, and ρ is a density of the crystal), in terms of the unstiffened constants $C_{\mu\nu}^E$ and the piezoelectric correction as obtained from eign values of the Christoffel tensor with the piezoelectric contributions included [25] are listed for eight modes measured. The relations

for ρV_i^2 were obtained from the general relations for C_3 symmetry by taking into account that for lead germanate the piezoelectric constants $e_{11} = e_{14} = 0$ [14] and by averaging over two domain states. Since the domains differ in the direction of the polar C-axis, the piezoelectric constants e_{14} , e_{15} , e_{13} and e_{33} (but not e_{11} and e_{22}) are of opposite sign in the two types of domains. For the modes $i = 6, 7$ and 8 the relation for ρV_i^2 in Table 1 are only accurate up to and including fourth power of the piezoelectric constants. In Table 2 the present experimental values of stiffened and unstiffened elastic constants of lead germanate at different temperatures (298, 323, 348, 373, 398, 423, 448, 473 and 513 K) calculated using the equations of ρV_i^2 from Table 1 and compared with Barsch et al. [21] values. Thermal expansion data required for calculating the density and ultrasonic path length versus temperature were taken from Iwasaki et al. [12]. Measurements are referred to right-handed orthogonal axes X_1 , X_2 and X_3 parallel to crystallographic directions [100], [120] and [001]. Hexagonal materials are transversely degenerate so that all directions in [001] are equivalent.

In Fig. 1 both the stiffened elastic constants $C_{\mu\nu}'$ (calculated by ignoring the piezoelectric correction terms in Table 1) and the unstiffened elastic constants $C_{\mu\nu}^E$ (after subtraction of piezoelectric stiffening) listed in Table 2 are plotted as a function of temperature using pulse superposition technique and compared with Barsch et al. results [21] using the same technique. The longitudinal moduli C_{11} and C_{33} were obtained from modes number 1, 4 and 7 plus 8, the shear moduli C_{44} and C_{66} are calculated from modes 3 and 5, and from modes 2 and 6, respectively. The off-diagonal modulus C_{12} was obtained from $C_{66} = (C_{11} - C_{12})/2$ and C_{13} from modes 7 and 8. The dielectric constant data required for the evaluation of the piezoelectric correction terms were obtained by extrapolating the measurements of Cline and Cross [17] on the frequency dependence of ϵ_{33} to 20 MHz. Room temperature piezoelectric constants as determined by Yamada et al. [14] are $e_{11} = 0.00$, $e_{14} = 0.00$, $e_{15} = 0.08$, $e_{22} = 0.09$, $e_{31} = 0.61$ and $e_{33} = 0.77$ C.m⁻². Since the only piezoelectric constants for which the temperature dependence has been measured are d_{31} and d_{22} , and since d_{22} is practically independent of temperature [14], it was assume that at all temperatures $e_{31} = e_{33}$, and that all other piezoelectric moduli are temperature dependence. The modulus $e = e_{31} = e_{33}$ was then determined from d_{31} by means of the relation $e = d_{31} / (S_{11}^E + S_{12}^E + S_{13}^E)$, where e and elastic compliances S_{11}^E , S_{12}^E and S_{13}^E were determined [14] self-consistently by interaction of the equations given in Table 1. Since the room temperature value of e obtained in this manner (0.158 C.m⁻²) is smaller than e_{31} and e_{33} of Yamada et al. [14]. All values of e were then multiplied by constant factor so as to bring the room temperature value into agreement with the average value $(e_{31} + e_{33})/2$ calculated from the values of Yamada et al. [14]. The dielectric constant data calculated from Uchida et al. [15] and the piezoelectric constants obtained in the manner outlined are listed in Table 3.

The elastic constants plotted in Fig. 1 as a function of temperature for unpoled lead germanate showed downward directed cusp-like anomalies for the moduli C_{11} , C_{33} , C_{12} and C_{13} , and a continuous monotonically decrease with the increase of temperature for the shear moduli C_{44} and $C_{66} = (C_{11} - C_{12})/2$. For C_{33} and C_{13} , the piezoelectric correction is large, so that the magnitude of the elastic anomalies is larger for unstiffened constants than stiffened ones. Since in the paraelectric phase the piezoelectric constant d_{31} is zero [14] the difference between the stiffened and unstiffened moduli should be negligibly small above the transition.

At room temperature, the uncertainty of the data arising from inconsistencies in the different modes and from errors in density and ultrasonic path length, and from piezoelectric correction amount to about 0.5 to 1%. Above room temperature the errors should not be significantly larger for C_{11} , C_{12} , C_{44} and C_{66} in the ferroelectric phase. Because of the unknown error of d_{31} used in the piezoelectric correction, and especially because of the simplifying assumption $e_{31} = e_{33}$ underlying the estimate of the piezoelectric correction term, the errors of C_{13}^E and C_{33}^E in the ferroelectric phase should be larger than the errors for other



moduli, and they may be expected to increase with the increase the temperature up to Curie point.

Discussion

The shape of the curves for the temperature dependence of the elastic moduli in Fig.1 suggests decomposing the moduli $C_{\mu\nu}^E$ additively into the usual linearly temperature dependence term $C_{\mu\nu}^0 = a_{\mu\nu} - b_{\mu\nu} T$ and into the cusp-like elastic anomaly $\Delta C_{\mu\nu}$ as given by:

$$C_{\mu\nu}^E = C_{\mu\nu}^0 + \Delta C_{\mu\nu} \quad (1)$$

Since it is apparent from Fig. 1 that the shear modulus $C_{66} = (C_{11}-C_{12})/2$ does not exhibit an elastic anomaly, which shows good agreement with Barsch et al. [21] results. It follows that both in the ferroelectric and in the paraelectric phases the following relation holds:

$$\Delta C_{11} = \Delta C_{12}, \quad (2-1)$$

Further one obtains from graphical analysis of the data in Fig.1 that the relationship:

$$\Delta C_{11} \Delta C_{33} = (\Delta C_{13})^2 \quad (2-2)$$

holds approximately in ferroelectric phase, but not in the paraelectric phases. The relative error of the $\Delta C_{\mu\nu}$ shows similar temperature dependence, because the absolute error of the piezoelectric correction increases with the increase of temperature. This suggests that the deviations of the $\Delta C_{\mu\nu}$ from Eq. (2-2) are primarily caused by systematic errors of the $\Delta C_{\mu\nu}$. Furthermore, C_{44} does not show an elastic anomaly, thus it is:

$$\Delta C_{44} = 0 \quad (2-3)$$

In both the ferroelectric and the paraelectric phases which show a good agreement with Barsch et al. results [21].

Barsch et al. [21] discussed in full detailed the reasons of elastic anomalies of lead germinate single crystal for both the ferroelectric phase (C^1_3) and the paraelectric phase (C_{3h}). The elastic anomaly in lead germanate could arise from a soft Raman active mode through the internal strain contributions of the elastic constants. All the Raman-active modes occur at the Brillouin zone center and so lead to displacive ferroelectric phase transition [18]. Miller and Axe [26] found that the elastic anomaly in β -quartz (space group D^1_6 or D^5_6) obeys the three Eqs. (2-1), (2-2) and (2-3), with regular terms $C_{\mu\nu}^0$ taken as constants. They showed that the elastic anomaly in β -quartz could arise from a soft Raman active mode through the internal strain contributions of the elastic constants. Axe and Shirane [27] have later established that the elastic anomaly in β -quartz could no longer be attributed to the internal strain contributions. They showed that the anharmonic contribution arising from virtual excitation of optical phonon pairs of wave vector q and $-q$ of an over damped soft mode could lead to elastic anomaly of the Eqs. (2-1), (2-2) and (2-3) if q is along the crystallographic C -direction [27]. Although the explanation of the elastic anomaly originally proposed by Miller and Axe [27] is not relevant for β -quartz it appears that the internal strain mechanism could account for the elastic anomaly in lead germinate.

Viswanathan [28] found that the gyrotropic anomaly in $Pb_5Ge_3O_{11}$ during phase transition lead to elastic anomalies on C_{11} , C_{33} , C_{12} , and C_{13} which suffered a dip at the transition temperature which show agreement with the present results and with Barsch et al. [21] results.

In ferroelectric phase the elastic anomaly for lead germanate obeys the three relations (2-1), (2-2) and (2-3), and since the lowest of the optical modes are soft and strongly temperature dependent [18,19], it is very likely that the elastic anomaly arise predominantly from soft mode through the internal strain mechanism. Barsch et al. [21] found that $Pb_5Ge_3O_{11}$ was the first material for which the linear acoustic-optic mode coupling mechanism proposed by Miller and Axe [26] is operative. Harmonic phonon-phonon interactions may also contribute to the elastic anomaly.

Generally, elastic moduli decrease with the increase of temperature, at least one of the coefficients must increase with temperature to achieve temperature compensation. Most materials soften at higher temperatures; the few with positive temperature coefficients generally show phase transition of some sort. Several of the elastic constants of $Pb_5Ge_3O_{11}$ increase with the increase of temperature just above Curie point between 453 and 473 K. C_{11} , C_{33} , C_{12} and C_{13} have positive temperature coefficients in this range. Since the Curie point of $Pb_5Ge_3O_{11}$ can be lowered to room temperature by doping the crystal by Si or Ba, the temperature compensation region can be moved to a more convenient working range. Unfortunately the 20 deg range of positive temperature coefficients is rather narrow and stiffnesses are changing rather rapidly. The piezoelectric coupling coefficients of lead germanate are also rather small for surface-wave devices [14], and losses tend to be high [13]. Thus it appears that the advantages of positive temperature coefficients to several elastic moduli are more than offset by other factors, and lead germanate, would be of little use as substrate material for ultrasonic surface wave devices. The discrepancies range for unstiffened elastic constant at different temperatures for this work comparing with Barsch et al. results [21] are from 1% for C_{33} and 5.3% for C_{13} .

Conclusions

From the present results, it can be concluded that the unpoled lead germanate shows an elastic anomalies for the elastic moduli C_{11} , C_{33} , C_{12} and C_{13} and a small continuous monotonically decrease for the shear moduli C_{44} and C_{66} with the increase of temperature. Several of the elastic constants of $Pb_5Ge_3O_{11}$ increase with the increase of temperature just above Curie point. The elastic anomalies for unstiffened elastic constants C_{33}^E and C_{13}^E are larger than the stiffened elastic constants C_{33}^C and C_{13}^C because the piezoelectric correction is large. Above Curie temperature (450 K) the difference between the stiffened and unstiffened elastic constants was small above transition temperature. The measured present results agreed with the previous results of Barsch et al. [21].

Acknowledgements

I am so grateful to Professor G.A. Saunders for many helpful discussions and much encouragement of this project.

References

1. Iwasaki, H.; Sugi, K.; Yamada, T. and Niizeki, N. (1971), $5PbO.3GeO_2$; A new ferroelectric, Appl. Phys. Lett. 18 (10): 444-445.
2. Nanamatsu, S.; Sugiyama, S.; Doi, K. and Kondo, Y. (1971), Ferroelectricity $Pb_5Ge_3O_{11}$, J. phys. Soc, Japan, 31:616-620.
3. Iwasaki, H. and Sugii, K. (1971), Optical Activity of Ferroelectric $5PbO.3GeO_2$ Single crystal, Appl. Phys Lett, 19(4): 92-93.
4. Mendricks, S.; Yue, X.; Pankrath, R. and Hesse, H., Kip D., (1999), Dynamic Properties of Multiple Grating Formation in Doped and Thermally Treated Lead Germanate, Appl. Phys. B68, 887-891.
5. Yue, X.; Mandricks, S.; Yi Hu, Hesse H. and Ki, D. (1998), Photorefractive Effect in Doped $Pb_5Ge_3O_{11}$ and in $(Pb_{1-x}Ba_x)_5Ge_3O_{11}$, J. Appl. Phys. 83(7): 3473-3479.
6. Trubitsyn, M.P.; Volnianskii, M.D., Ermakov A.S., and Linnik V.G, (1999), Ferroelectric Phase Transition in Lead Germanate $Pb_5Ge_3O_{11}$ Studied by ESR of Cd^{+3} Prope, Condensed Matter Phys. 2 (4):677-684.
7. Newnham, R.E. and Gross, L.E. (1974), Ambidextrous Crystals, Endeavour 23, 18-23.



8. Shaldin, Yu.V., Bush A.A., Matyjasik S., and Rabadanov M.Kh., (2005), Characteristic of Spontaneous Polarization in $Pb_5Ge_3O_{11}$ Crystals, *Crystallography Reports* 50 (5): 836-842.
9. Mirsa, N.K.; Sati, R. and Choudhary, R.N.P. (1996), Phase Transition in Modified Lead Germanate , *Ferroelectrics*, 189 1, 39-42.
10. Molak, A.; Koralewski, M.; Saunders, G.A. and Juszczyk, W. (2005), Effect of Uniaxial Pressure on the Ferroelectric Phase Transition in $Pb_5Ge_3O_{11}$: Ba Crystal, *Acta Phys. Pol. A* 108 (3): 513-520.
11. Nanda Gowswami, M.L.; Choudhary, R.N.P. and Mahapatra, P.K.,(1999), Ferroelectric Phase Transition in Modified Lead Germanate, *Ferroelectrics* 227(1): 175-187.
12. Iwasaki ,H.; Miyazawa, S.; Koizumi ,H.; Sugii ,K. and Niizeki, N. J. (1972), Ferroelectric and Optical Properties of $Pb_5Ge_3O_{11}$ and its Amorphous Compound $Pb_5Ge_2SiO_{11}$, *Appl. Phys.* 43(12): 4907-4915.
13. Ohmachi, Y. and Uchida,N. J. (1972), Acousto- Optic Properties of Single Crystal $5PbO.3GeO_2$, *Appl. Phys.*43, 3583-3584.
14. Yamada, T.; Iwasaki ,H. and Niizeki, N., J. (1972), Elastic and Piezoelectric Properties of Ferroelectric $5PbO.3GeO_2$ Crystals, *Appl. Phys.* 433, 771-775.
15. Uchida, N.; Saku, T.; Iwasaki H., and Onuki K., J. (1972), Electro-Optic Properties of Ferroelectric $5PbO.3GeO_2$ Single Crystal, *Appl. Phys.* 43 (12): 4933-4936.
16. Bichard, V.M.; Davies, P.H.; Hulme, K.F.; Jones, G.R. and Robertson, D.S., (1972), Electro-Optic Measurements on Lithium Germanate ($Li_2O.GeO_2$) and Lead Germanate $Pb_5Ge_3O_{11}$, *J. Phys. D Appl. Phys.* 5 (11): 2124-2128.
17. Cross, L.E. and Cline, T.W., (1976), Contribution to the Dielectric Response from Charged Domain Walls in Ferroelectric $Pb_5Ge_3O_{11}$, *Ferroelectrics* 11, 333-336.
18. Ryan, J.F. and Hisano, K. (1973), Raman Scattering and Ferroelectric Phase Transition in $5PbO.3GeO_2$, *J. Phys. C. Solid State Phys.* 6, 566-574.
19. Burns, G. and Scott, B.A. (1972), Soft Optic Phonon Mode in Ferroelectric $Pb_5Ge_3O_{11}$, *Phys. Lett. A* 39, 177-179.
20. AlMummar, I.J.; Saunders, G.A. (1986), Acoustic Symmetry and Vibrational Anharmonicity of Rhombohedral $Pb_5Ge_3O_{11}$ and $Pb_{4.7}Ba_{0.3}Ge_3O_{11}$, *Phys. Rev. B* 34(6): 4304-4315.
21. Barsch, G.R.;Bonczar, L.J. and Newnham, R.E. (1975), Elastic Constants of $Pb_5Ge_3O_{11}$ from 25 to 240⁰C , *Phys. Stat. Sol. A* 29, 241-250.
22. Sugii, K.; Iwasaki, H. and Migazawa, S. (1971), Crystal Growth and Some Properties of $5PbO.3GeO_2$ Single Crystals, *Mater Res. Bull.*6, 503-512.
23. Al-Mummar, I.J. (1985), Ultrasonic Studies of the Elastic Properties of Lead Germanate Under Pressure, M.Sc. Thesis, Bath University, Bath, UK.
24. Mc Skimin, H.J. (1961), Pulse Superposition Method for Measuring Ultrasonic Wave Velocities in Solids, *J. Acoust. Soc. Am.* 33 1, 12-16.
25. Kyame, J.J. (1949), Wave Propagation in Piezoelectric Crystals, *J. Acous. Soc. Am.*21, 159-167.
26. Miller, P.B. and Axe ,J.D. (1967), Study of Optical and Elastic Properties of α - β Quartz, *Phys. Rev.*163, 924-929.
27. Axe, J.D. and Shirane, G. (1970), Study of the α - β Quartz Phase Transformation by Inelastic Neutron Scattering, *Phys. Rev.* B1, 342-348.
28. Viswanathan, K.S. (1994), Elastic and Gyrotropic Anomalies and Acoustic Activity in Lead Germanate, *Can. J. Phys.* 72 9-10, 568-573.

Table(1): Relation between ultrasonic velocities (V_i), stiffened elastic constants ($C_{\mu\nu}'$), and unstiffened elastic constants ($C_{\mu\nu}^E$).

Mode i	Direction of		ρV_i^2
	Propagation	Polarization	
1	X_1	X_1	C_{11}^E
2	X_1	X_2	$C_{66}' = C_{66}^E + e_{22}^2/\epsilon_{11}^S$
3	X_1	X_3	$C_{44}' = C_{44}^E + e_{15}^2/\epsilon_{11}^S$
4	X_3	X_3	$C_{33}' = C_{33}^E + e_{33}^2/\epsilon_{33}^S$
5	X_3	X_1	C_{44}^E
6	45° to X_1, X_3	X_2	$2(C_{44}^E + C_{66}^E) + V^2 - \Delta$
7	45° to X_1, X_3	Quasi longitudinal	$[A + (B^2 + 4C)^{1/2}]/4$
8	45° to X_1, X_3	Quasi shear	$[A - (B^2 + 4C)^{1/2}]/4$

$$A = (C_{11}^E + C_{33}^E + 2C_{44}^E) + 2(U^2 + V^2 + W^2) + 2\Delta$$

$$B = (C_{11}^E - C_{33}^E - 2C_{66}^E) + 2(U^2 - V^2 + W^2) - 2\Delta C$$

$$C = -(C_{11}^E + C_{66}^E + 2U^2)(C_{33}^E - C_{66}^E - 2V^2 + 2W^2) + (C_{13}^E + C_{44}^E + 2VW)^2 + 4V^2(V^2 + W^2)$$

$$\Delta = 2V^2 [(C_{11}^E - C_{66}^E + 2U^2)W^2 + (C_{33}^E - C_{66}^E - 2V^2 + 2W^2)V^2 - 2(C_{13}^E + C_{44}^E + 2VW)VW] / [(C_{11}^E - C_{66}^E + 2U^2)(C_{33}^E - C_{66}^E - 2V^2 + 2W^2) - (C_{13}^E + C_{44}^E + 2VW)^2]$$

$$U^2 = 2(e_{22})^2 / (\epsilon_{11}^S + \epsilon_{33}^S)$$

$$V^2 = (e_{15} + e_{31})^2 / 2(\epsilon_{11}^S + \epsilon_{33}^S)$$

$$W^2 = (2e_{15} + e_{33})^2 / 2(\epsilon_{11}^S + \epsilon_{33}^S)$$

Table 2. Experimental values of stiffened elastic constants ($C_{\mu\nu}'$) and unstiffened elastic constants ($C_{\mu\nu}^E$) in 10^{10} N/m² at different temperatures (calculated from ρV_i^2 in Table 1).

T (K)	C_{11}^E	C_{11}'	C_{12}^E	C_{12}'	C_{13}^E	C_{13}'	C_{33}^E	C_{33}'	C_{44}^E	C_{44}'	C_{66}^E	C_{66}'
298	6.78*	6.78*	2.52*	2.50*	1.79*	1.92*	9.30*	9.43*	2.24*	2.20*	2.13*	2.14*
	6.80†	–	2.57†	–	1.89†	–	9.42†	9.55†	2.23†	2.21†	2.11†	2.12†
323	6.72*	6.72*	2.48*	2.47*	1.77*	1.90*	9.24*	9.40*	2.24*	2.20*	2.12*	2.13*
	6.75†	–	2.55†	–	1.87†	–	9.35†	–	2.23†	–	2.10†	–
348	6.67*	6.67*	2.46*	2.45*	1.75*	1.89*	9.18*	9.38*	2.23*	2.195*	2.11*	2.125*
	6.71†	–	2.54†	–	1.85†	–	9.28†	–	2.22†	–	2.09†	–
373	6.61*	6.61*	2.44*	2.41*	1.72*	1.88*	9.15*	9.32*	2.23*	2.19*	2.210*	2.12*
	6.66†	–	2.52†	–	1.83†	–	9.20†	9.42†	2.22†	2.20†	2.07†	2.07†
398	6.57*	6.57*	2.41*	2.39*	1.69*	1.84*	9.01*	9.03*	2.22*	2.197*	2.09*	2.1*
	6.61†	–	2.50†	–	1.79†	–	9.10†	–	2.21†	–	2.06†	–
423	6.51*	6.51*	2.38*	2.37*	1.66*	1.78*	8.78*	8.80*	2.22*	2.186*	2.085*	2.09*
	6.55†	–	2.47†	–	1.76†	–	8.97†	–	2.21†	–	2.04†	–
448	6.36*	6.36*	2.34*	2.34*	1.57*	1.73*	8.84*	8.62*	2.21*	2.173*	2.07*	2.08*
	6.34†	–	2.41†	–	1.67†	–	8.73†	–	2.20†	–	2.01†	–
473	6.50*	6.50*	–	2.40*	–	1.76*	–	9.01*	2.20*	2.163*	–	2.07*
	6.52†	–	–	–	–	–	–	9.06†	–	2.167†	–	2.00†
513	6.49*	6.49*	–	2.44*	–	1.64*	–	8.98*	2.20*	2.151*	–	2.05*
	6.50†	–	–	–	–	–	–	8.98†	–	2.15†	–	1.99†

* Present experimental results

† Barsch et al. results [21]

Table(3): Dielectric constants ϵ_{33} (calculated from data of Cross and Cline [17] and piezoelectric constants e (calculated from data for d_{31} of Yamada et al. [14]) by using the assumption ($e = e_{31} = e_{33}$) versus temperature.

T (K)	Dielectric constants (ϵ_{33})	Piezoelectric constants (e) (C.m ⁻²)
298	40	0.690
323	44	0.764
348	50	0.842
373	61	0.941
398	78	1.099
423	133	1.432
448	2100	5.903

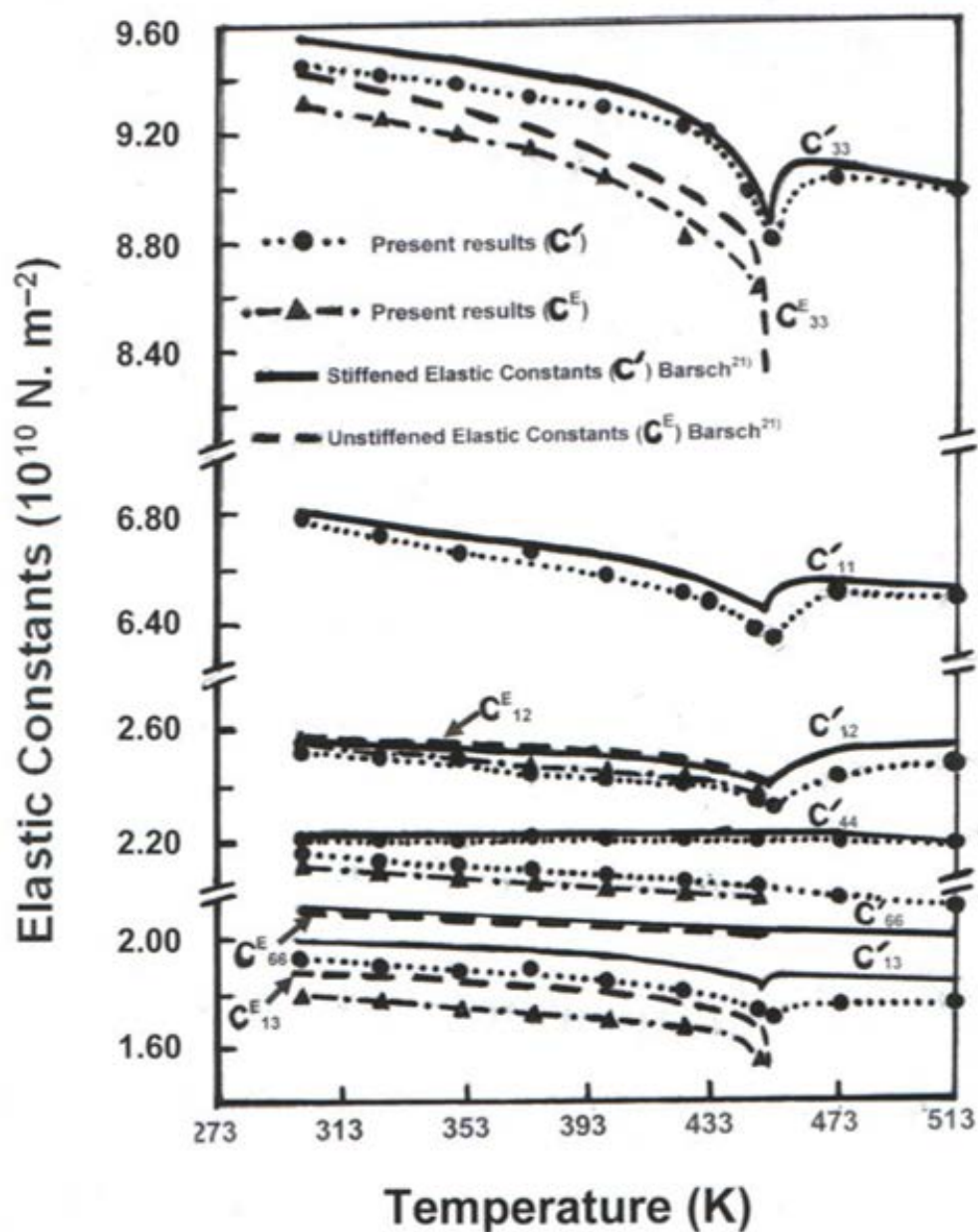


Fig. (1): Experimental results of elastic constants for lead germanate ($\text{Pb}_5\text{Ge}_3\text{O}_{11}$) as a function of temperature, where (closed circles $\bullet\bullet\bullet\bullet\bullet$) represents the present experimental results of stiffened elastic constants (C' ignoring piezoelectric stiffening) and (closed triangles $\bullet-\blacktriangle-\bullet$) represents present experimental results of unstiffened elastic constants (C^E after subtracting piezoelectric stiffening) compared with Barsch et al. results [21] for which the solid lines is the stiffened elastic constants (C') and the dashed lines is unstiffened elastic constants (C^E).

السلوك المرن لجيرمانيت الرصاص بالقرب من درجة حرارة الانتقال

اكرام جميل عبد الغني

قسم الفيزياء ، كلية التربية - ابن الهيثم ، جامعة بغداد

استلم البحث في : 15 نيسان 2012 قبل البحث في : 9 كانون الاول 2012

الخلاصة

قياس جميع ثوابت المرنة المصلّبة وغير المصلّبة لبلورة جيرمانيت الرصاص الأحادية بدرجات حرارة تتراوح من درجة حرارة الغرفة 298K الى 513K باستخدام تقنية التراكب النبضي فوق الصوتي. وقد استخدم التصحيح لعوامل التصلب الكهروضغطية بعد طرحها من ثوابت المرنة المصلّبة وذلك لحساب ثوابت المرنة غير المصلّبة. وقد بيّنت النتائج ان معاملات المرنة لجيرمانيت الرصاص (C_{11} , C_{33} , C_{12} , C_{13} , C_{44} and C_{66}) تتناقص بزيادة درجة الحرارة. اذ تعاني معاملات المرنة الآتية C_{11} , C_{33} , C_{12} and C_{13} من انخفاض شديد عند درجة حرارة الانتقال (450K) الا انها تزداد بزيادة درجة الحرارة مباشرة فوق درجة حرارة الانتقال (كبيوري) بين 453K و 473K وذلك بسبب كون معاملات درجة الحرارة ضمن هذا المدى تكون موجبة ثم تتناقص بشكل طفيف (عدا C_{12} يزداد قليلا) بين 473K و 513K. اما ثابت المرنة القصّي C_{44} فإنه يزداد بصورة تدريجية بطيئة الى نقطة الانتقال وبعدها يبدأ بالتناقص الضئيل التدريجي. اما ثابت المرنة القصي C_{66} فإنه يتناقص تدريجيا وباستمرار مع زيادة درجة الحرارة. قورنت نتائج هذا البحث مع النتائج العملية للبحوث المنشورة سابقا.

الكلمات المفتاحية: جيرمانيت الرصاص ، المرنة، درجة حرارة الانتقال ، النشاط البصري، البلورة الكهروضغطية.